EURASIP Journal on Wireless Communications and Networking

RESEARCH Open Access

Uplink RIS-assisted NOMA/OMA networks: a theoretical study

Slimane Benmahmoud[1], Abdelhalim Rabehi[2], El-Hadi Meftah[3], Abdelaziz Rabehi[2], Xiaofan He[4] and Takele Ferede Agajie[5*]

*Correspondence:
takele_ferede@dmu.edu.et

[1] Department of Electronic Engineering, M'sila University, 28000 M'sila, Algeria
[2] Laboratory of Telecommunications and Smart Systems, Faculty of Science and Technology, University of Djelfa, PO Box 3117, Djelfa, Algeria
[3] Department of Electronics, Faculty of Electrical Engineering, USTHB, 16111 Algiers, Algeria
[4] Electronic Information School, Wuhan University, Wuhan 430072, China
[5] Department of Electrical and Computer Engineering, Faculty of Technology, Debre Markos University, P. BOX 269, Debre Markos, Ethiopia

Abstract

In this paper, we have investigated the outage probabilities (OPs) and the ergodic rates (ERs) of uplink reconfigurable intelligent surface (RIS)-assisted non-orthogonal and orthogonal multiple-access (NOMA and OMA) networks. Particularly, we have tackled a challenging scenario in which both user equipments (UEs) need assistance from the same RIS unit to communicate with the base station (BS). We have modeled all the UEs→RIS and RIS→BS links as Nakagami-*m* variates. To assess the performance of these networks, we have derived the necessary statistics for the effective channel gain of the reflected (UE→RIS→BS) link for the randomly phase-shifted UE, while adopting its already-existing counterpart statistics for the coherently phase-shifted one. On the basis of that, we have derived closed-form expressions for the OPs and the ERs for both RIS-assisted NOMA and OMA schemes. Finally, to get further insights on these results, we have elaborated on the high signal-to-noise ratio (SNR) regime.

Keywords: Reconfigurable intelligent surface (RIS), Orthogonal/non-orthogonal multiple-access (OMA/NOMA), User equipment (UE), Smart radio environments (SREs), Outage probability, Ergodic rate

1 Introduction

One of the basic postulates in conventional communication theory is that the wireless environment is naturally random and unmodifiable. This means that we lack control over it, particularly with regards to the reflection and refraction phenomena of the radio waves. As a result when designing a wireless communication system, we must adapt to it through the design of sophisticated transceivers. However, the concept of smart radio environments (SREs) or "Wireless 2.0" [1] provides a contrasting perspective by allowing to manipulate the behavior of the radio waves after scattering from objects. The aim is to maximize the power of reflection toward the desired user(s) while minimizing it in unwanted directions. Reconfigurable intelligent surfaces (RISs) [2–7] have appeared as a technology enabler to realize the concept of SREs. RISs are thus used as an energy/spectral efficient and low-cost solution to astutely adapt the propagation environment aiming to improve the reception's reliability [2, 3, 8, 9]. A RIS consists of a 2D planar surface composed of a large number of reconfigurable inexpensive passive elements on

© The Author(s) 2026. **Open Access** This article is licensed under a Creative Commons Attribution 4.0 International License, which permits use, sharing, adaptation, distribution and reproduction in any medium or format, as long as you give appropriate credit to the original author(s) and the source, provide a link to the Creative Commons licence, and indicate if changes were made. The images or other third party material in this article are included in the article's Creative Commons licence, unless indicated otherwise in a credit line to the material. If material is not included in the article's Creative Commons licence and your intended use is not permitted by statutory regulation or exceeds the permitted use, you will need to obtain permission directly from the copyright holder. To view a copy of this licence, visit http://creativecommons.org/licenses/by/4.0/.

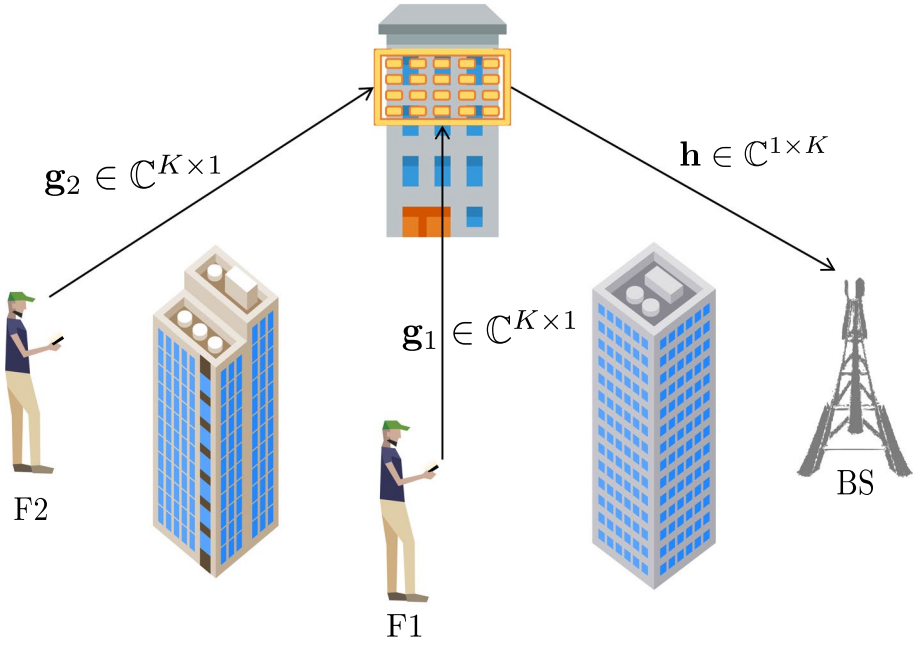

Fig. 1 A schematic diagram illustrating the uplink scenario studied in the manuscript. Two single-antenna user equipments (F1 and F2) are assisted by a single reconfigurable intelligent surface (RIS) composed of *K* reflecting elements and communicate with a single-antenna base station (BS). Direct UE–BS links are assumed blocked

3 System and channel models

We examine an uplink RIS-aided NOMA/OMA network where two single-antenna UEs (denoted by F1 and F2) establish communications with a single-antenna BS via the RIS, as shown in Fig. 1. Direct links between the UEs and the BS are assumed absent, primarily attributed to obstructive objects causing blockage. More specifically, both F1 and F2 need help from the RIS to communicate with the BS. The RIS has K reflecting elements, and its reflection-coefficients and phase-shifts matrix is denoted by $\mathbf{\Theta} = \text{diag}\left(\beta_1 e^{j\theta_1}, \beta_2 e^{j\theta_2}, \cdots, \beta_K e^{j\theta_K}\right)$, where $\beta_k \in [0,1]$ is the amplitude-reflection coefficient and $\theta_k \in [0, 2\pi)$ is the phase-shift variable of the k^{th} element that can be adjusted by the RIS ($k = 1, 2, \cdots, K$). We assume, without loss of generality, that $\beta_k = \beta$, $\forall k \in \{1, 2, \cdots, K\}$ [35].

The signal y received at the BS is given by

$$y = d_3^{-\frac{\alpha_3}{2}} \sqrt{P} \sum_{i=1}^{2} d_i^{-\frac{\alpha_i}{2}} (\mathbf{h}\Theta\mathbf{g}_i) s_i + n, \; i \in \{1, 2\}, \tag{1}$$

where $\mathbf{g}_1 \in \mathbb{C}^{K\times 1}$, $\mathbf{g}_2 \in \mathbb{C}^{K\times 1}$, and $\mathbf{h} \in \mathbb{C}^{1\times K}$ are the small-scale fading vectors of the F1→RIS, F2→RIS, and RIS→BS links, respectively[1]. Particularly, they are $\mathbf{g}_1 = [g_{1,1}, g_{1,2}, ..., g_{1,K}]^T$, $\mathbf{g}_2 = [g_{2,1}, g_{2,2}, ..., g_{2,K}]^T$, and $\mathbf{h} = [h_1, h_2, ..., h_K]$, respectively.

[1] The Nakagami-m model plays a central role in Lemma 1 because it offers analytically manageable expressions for the product of random variables. The parameter ξ a, determined by m_Y and m_Z, provides direct control over the non-centrality parameter of the chi-square approximation, enabling accurate modeling under a wide range of propagation conditions.

1 Lemma 1

[15] *Let* $\{Y_k\}_{k=1}^{K}$ *be a sequence of i.i.d RVs for which* $|Y_k| \sim$ Nakagami$(m_Y, 1)$ *and* $\{Z_k\}_{k=1}^{K}$ *be a sequence of i.i.d RVs for which* $|Z_k| \sim$ Nakagami$(m_Z, 1)$. *Let* $\xi = \frac{1}{m_Y m_Z}\left(\frac{\Gamma\left(m_Y+\frac{1}{2}\right)}{\Gamma(m_Y)}\right)^2\left(\frac{\Gamma\left(m_Z+\frac{1}{2}\right)}{\Gamma(m_Z)}\right)^2$. *When K is large* (*i.e*, $K >> 0$), *the RV*

$$S = \frac{\left(\sum_{k=1}^{K} Y_k Z_k\right)^2}{K(1-\xi)}, \tag{5}$$

has a tendency to follow a non-central chi-square distribution as $S \sim \chi'^2_1\left(\frac{K\xi}{1-\xi}\right)$.

4.1 Key results

1 Lemma 2

Let $\{Y_k\}_{k=1}^{K}$ *be a sequence of i.i.d RVs for which* $|Y_k| \sim$ Nakagami(m_Y, Ω_Y) *and* $\{Z_k\}_{k=1}^{K}$ *be a sequence of i.i.d RVs for which* $|Z_k| \sim$ Nakagami(m_Z, Ω_Z). *Let* ϕ_k *be a uniformly distributed RV over the interval* $[0, 2\pi)$. *When K is large* (*i.e*, $K >> 0$), *the RV*

$$S = \left|\sum_{k=1}^{K} e^{j\phi_k} Y_k Z_k\right|^2, \tag{6}$$

tends to follow an exponential distribution as $S \sim \text{Exp}\left(\frac{1}{K}\right)$.

1 ***Proof***

Resorting to [16], the summation $S_1 = \sum_{k=1}^{K} e^{j\phi_k} Y_k Z_k$ *in (6) can be approximated, according to the central limit theorem (CLT), to match a complex Gaussian distribution* $S_1 \sim \mathcal{CN}(0, K)$. *Then, the RV* $S_2 = |S_1| \sim \text{Rayleigh}\left(\sqrt{\frac{K}{2}}\right)$. *Finally,* $S = S_2^2$ *is a one-to-one transformation with an inverse* $S_2 = g^{-1}(S) = \sqrt{S}$ *and a Jacobian* $\frac{dS_2}{dS} = \frac{1}{2\sqrt{S}}$. *Therefore, by the transformation technique, it is clear that the RV S is exponentially distributed with a mean K. When going through different steps in this proof, one can easily see that the result in Lemma 2 relies on three key basic conditions: the phase shifts* ϕ_k *are i.i.d and uniformly distributed over* $[0, 2\pi)$*; the channel amplitudes* $|Y_k|$ *and* $|Z_k|$ *are independent of* ϕ_k*; and the value of K is sufficiently large to justify the use of the CLT.*

□

1 Theorem 1

Let and $X \sim \text{Exp}(\lambda)$ *be two independent RVs. Let* $a, b, c > 0$. *Then, the CDF* $F_Z(z)$ *of* $tY \sim \chi_1^{'2}(\zeta)$ *he RV* $Z = \frac{aY}{bX+c}$ *is given by*

$$F_Z(z) = \frac{e^{\frac{\lambda}{b}-\frac{\zeta}{2}}}{\sqrt{\frac{2a\lambda}{bz}}} \sum_{i=0}^{+\infty}\sum_{j=0}^{+\infty} \frac{\zeta^i(-1)^j\Gamma(i+j+\frac{3}{2},\frac{\lambda c}{b})}{i!2^i j!(i+j+\frac{1}{2})\Gamma(i+\frac{1}{2})(\frac{2a\lambda}{bz})^{(i+j)}}. \tag{7}$$

1 ***Proof***

A detailed proof is provided in Appendix A.

□

1 Theorem 2

Let $Y \sim \chi_1^{'2}(\zeta)$ *and* $X \sim \text{Exp}(\lambda)$ *be two independent RVs. Let* $a, b, c, \gamma_1, \gamma_2 > 0$. *Then, the probability* $P = \Pr\left\{\frac{aY}{bX+c} \geq \gamma_1, \frac{b}{c}X \geq \gamma_2\right\}$ *is given by*

$$\begin{aligned} P =& e^{\left(\frac{-\zeta}{2}+\frac{\lambda}{b}\right)} \times \left(e^{-\left(\frac{\lambda c\gamma_2}{b}+\frac{\lambda c}{ba}\right)} \sum_{i=0}^{+\infty} \frac{\zeta^i}{i!2^i} \right. \\ &\left. + \frac{1}{\sqrt{\frac{2a\lambda}{b\gamma_1}}} \sum_{i=0}^{+\infty}\sum_{j=0}^{+\infty} \frac{\zeta^i(-1)^j\Gamma\left(i+j+\frac{3}{2},\frac{\lambda c}{2}(\gamma_2+1)\right)}{i!j!2^i\left(i+j+\frac{1}{2}\right)\Gamma\left(i+\frac{1}{2}\right)\left(\frac{2a\lambda}{b\gamma_1}\right)^{(i+j)}} \right). \end{aligned} \tag{8}$$

1 ***Proof***

A detailed proof is provided in Appendix B.

□

1 Theorem 3

(*The expected value of* $Z = \log_2\left(1+\frac{aY}{bX+c}\right)$)

Let $Y \sim \chi_1^{'2}(\lambda_Y)$ *and* $X \sim \text{Exp}(\lambda_X)$ *be two independent RVs. Let* $a, b, c > 0$. *Then, the expected value of the RV* $Z = \log_2\left(1+\frac{aY}{bX+c}\right)$, $\mathbb{E}(Z)$ *is given by*

$$\begin{aligned} \mathbb{E}(Z) \approx& -\frac{\lambda_X}{\ln 2} e^{\left(\frac{ac\lambda_X}{b}-\frac{\lambda_Y}{2}\right)} \\ &\times \sum_{i=0}^{+\infty}\sum_{l=1}^{u_3} \frac{\lambda_Y^i\, y_{3,l}^{\left(i+\frac{1}{2}\right)} e^{\left(\frac{ac\lambda_X}{b}+\frac{1}{2}\right)y_{3,l}} \text{Ei}\left(-\lambda_X(\frac{ay_{3,l}}{b}+\frac{ac}{b})\right)}{i!2^{2i+\frac{1}{2}}\Gamma\left(i+\frac{1}{2}\right)(u_3+1)^2\left(L_{u_3+1}\left(y_{3,l}\right)\right)^2}, \end{aligned} \tag{9}$$

where u_3 is the number of nodes utilized in the Gauss-Laguerre quadrature technique, and $y_{3,l}$ is the lth root of Laguerre polynomial $L_{u_3}(y)$.

1 ***Proof***

The detailed proof is provided in Appendix C.

□

1 ***Remark 1***

The infinite series in Theorems 1–3 converge absolutely because the factorial terms in the denominators (i!, j!) guarantee fast decay of successive terms. For practical computation, truncating the series at $i, j \leq 20$ is sufficient, yielding a relative error below 10^{-6} for Theorems 1–2 and below 10^{-4} for Theorem 3). In Theorem 3, the Gauss–Laguerre quadrature achieves stable convergence with $u_3 \geq 10$ nodes. All series remain numerically stable for positive parameter values, ensuring reliable implementation.

1 Theorem 4

(*The expected value of $Z = \log_2(1 + aX)$ with $X \sim \text{Exp}(\lambda_X)$, and $a > 0$*)

Let $X \sim \text{Exp}(\lambda_X)$, and $a > 0$. Then, the expected value of the RV $Z = \log_2(1 + aX)$, $\mathbb{E}(Z)$ is given by

$$\mathbb{E}(Z) \approx \lambda_X \sum_{l=1}^{u_4} \frac{x_{4,l} e^{\left(\frac{\lambda_X - 1}{\lambda_X}\right) x_{4,l}} \log_2\left(1 + a x_{4,l}\right)}{\left(u_{4,l} + 1\right)^2 \left(L_{u_4+1}\left(x_{4,l}\right)\right)^2}, \tag{10}$$

where u_4 is the number of nodes for the Gauss-Laguerre quadrature, and $x_{4,l}$ is the lth root of Laguerre polynomial $L_{u_4}(x)$.

1 ***Proof***

First, $\mathbb{E}(Z)$ is given by

$$\mathbb{E}(Z) = \mathbb{E}\left(\log_2(1 + aX)\right), \tag{11}$$

which can be expressed as

$$\begin{aligned} \mathbb{E}(Z) &= \int_0^{+\infty} \log_2(1 + ax) f_X(x) dx \\ &= \lambda_X \int_0^{+\infty} e^{-\lambda_X x} \log_2(1 + ax) dx. \end{aligned} \tag{12}$$

The integral in (12) can be approximated employing the Gauss-Laguerre quadrature, to get the result in (10). □

1 Theorem 5

(*The expected value of* $Z = \log_2(1 + aY)$ *with* $Y \sim \chi_1^{'2}(\lambda_Y)$, *and* $a > 0$)

Let $Y \sim \chi_1^{'2}(\lambda_Y)$, *and* $a > 0$. *Then, the expected value of* $Z = \log_2(1 + aY)$, $\mathbb{E}(Z)$ *is given by*

$$\begin{aligned}\mathbb{E}(Z) \approx & \frac{\lambda_Y^{\frac{1}{4}} e^{-\frac{\lambda_Y}{2}}}{2} \\ & \times \sum_{l=1}^{u_5} \frac{y_{5,l}^{\frac{3}{4}} e^{\frac{y_{5,l}}{2}} I_{-\frac{1}{2}}\left(\sqrt{\lambda_Y y_{5,l}}\right) \log_2\left(1 + a\rho y_{5,l}\right)}{\left(u_{5,l}+1\right)^2 \left(L_{u_5+1}\left(y_{5,l}\right)\right)^2},\end{aligned} \tag{13}$$

where u_5 *represents the number of nodes utilized in the Gauss-Laguerre quadrature technique, and* $y_{5,l}$ *is the lth root of Laguerre polynomial* $L_{u_5}(y)$.

1 ***Proof***

$\mathbb{E}(Z)$ *is re-expressed as*

$$\begin{aligned}\mathbb{E}(Z) &= \int_0^{+\infty} \log_2\left(1 + ay\right) f_Y(y) dy \\ &= \frac{\lambda_Y^{\frac{1}{4}} e^{-\frac{\lambda_Y}{2}}}{2} \\ &\times \int_0^{+\infty} e^{-\frac{y}{2}} y^{-\frac{1}{4}} I_{-\frac{1}{2}}\left(\sqrt{\lambda_Y y}\right) \log(1 + ay) dy.\end{aligned} \tag{14}$$

The integral in (14) can be approximated using the Gauss-Laguerre quadrature, to get the result in (13). □

1 ***Remark 2***

The exponential approximation in Lemma 2 holds under the conditions specified in its proof and becomes exact as $K \to \infty$ *by virtue of the CLT. The Gauss–Laguerre quadrature approximation used in Theorems 3–5 exhibits exponential convergence for smooth integrands. The approximation error decreases rapidly as the number of nodes u increases, and choosing* $u \geq 10$ *provides relative errors below* 10^{-4} *for typical parameter settings, which is adequate for practical use.*

5 Results and discussion

In this section, leveraging the distributions and key results developed in Sect. 4, we derive closed-form expressions for the outage probabilities and ergodic rates of the considered uplink RIS-assisted NOMA and OMA systems, and provide their high-SNR asymptotic characterizations.

5.1 RIS-NOMA case

5.1.1 OPs

Considering the SINR in (3) and the SNR in (4) described in Section 3, the OPs of F1 and F2, corresponding to thresholds $\tilde{\gamma}_1$ and $\tilde{\gamma}_2$, are expressed as

$$\mathbb{P}_1(\tilde{\gamma}_1) = \Pr\{\Lambda_1 \leq \tilde{\gamma}_1\}, \tag{15}$$

and

$$\mathbb{P}_2(\tilde{\gamma}_1, \tilde{\gamma}_2) = 1 - \Pr\{\Lambda_1 \geq \tilde{\gamma}_1, \Lambda_2 \geq \tilde{\gamma}_2\}, \tag{16}$$

respectively, where $\tilde{\gamma}_1 = 2^{\tilde{R}_1} - 1$ and $\tilde{\gamma}_2 = 2^{\tilde{R}_2} - 1$ with $\tilde{R}_1$ and $\tilde{R}_2$ being the target rates of F1 and F2, respectively.

Considering Lemma 1, Lemma 2, Theorem 1, and Theorem 2 from Sect. 4.1, the OPs $\mathbb{P}_1(\tilde{\gamma}_1)$ and $\mathbb{P}_2(\tilde{\gamma}_1, \tilde{\gamma}_2)$ are expressed as

$$\begin{aligned}\mathbb{P}_1(\tilde{\gamma}_1) = &\frac{e^{\left(\frac{1}{Kb} - \frac{\lambda}{2}\right)}}{\sqrt{\frac{2a}{Kb\tilde{\gamma}_1}}} \\ &\times \sum_{i=0}^{+\infty}\sum_{j=0}^{+\infty} \frac{\lambda^i (-1)^j \Gamma\left(i+j+\frac{3}{2}, \frac{1}{Kb\rho'}\right)}{i!j!2^i \left(i+j+\frac{1}{2}\right)\Gamma\left(i+\frac{1}{2}\right)\left(\frac{2a}{Kb\tilde{\gamma}_1}\right)^{(i+j)}},\end{aligned} \tag{17}$$

and

$$\begin{aligned}\mathbb{P}_2(\tilde{\gamma}_1, \tilde{\gamma}_2) = 1 - e^{\left(\frac{1}{Kb} - \frac{\lambda}{2}\right)} \Bigg(&e^{-\left(\frac{\tilde{\gamma}_2}{Kb\rho'} + \frac{1}{Kba\rho'}\right)} \sum_{i=0}^{+\infty} \frac{\lambda^i}{i!2^i} \\ &+ \frac{1}{\sqrt{\frac{2a}{Kb\tilde{\gamma}_1}}} \\ &\times \sum_{i=0}^{+\infty}\sum_{j=0}^{+\infty} \frac{\lambda^i (-1)^j \Gamma\left(i+j+\frac{3}{2}, \frac{\tilde{\gamma}_2+1}{Kb\rho'}\right)}{i!j!2^i \left(i+j+\frac{1}{2}\right)\Gamma\left(i+\frac{1}{2}\right)\left(\frac{2a}{Kb\tilde{\gamma}_1}\right)^{(i+j)}} \Bigg),\end{aligned} \tag{18}$$

respectively, where

$$\begin{cases} a = d_1^{-\alpha_1} d_3^{-\alpha_3} \beta^2 K(1-\xi), & \text{(19a)} \\ b = d_2^{-\alpha_2} d_3^{-\alpha_3} \beta^2, & \text{(19b)} \\ \lambda = \frac{K\xi}{1-\xi}, & \text{(19c)} \end{cases}$$

with $\xi = \frac{1}{m_3 m_1} \left(\frac{\Gamma\left(m_3+\frac{1}{2}\right)}{\Gamma(m_3)}\right)^2 \left(\frac{\Gamma\left(m_1+\frac{1}{2}\right)}{\Gamma(m_1)}\right)^2$.

5.1.2 ERs

Considering the SINR in (3) and the SNR (4) described in Section 3, the ERs of F1 and F2 are given by

$$R_1 = \mathbb{E}\big(\log_2(1+\Lambda_1)\big), \tag{20}$$

and

$$R_2 = \mathbb{E}\big(\log_2(1+\Lambda_2)\big), \tag{21}$$

respectively.

Considering Lemma 1, Lemma 2, Theorem 3, and Theorem 4 from Subsection 4.1, R_1 and R_2 are expressed as

$$\begin{aligned} R_1 = &-\frac{1}{K\ln 2}\, e^{\left(\frac{a}{Kb\rho'}-\frac{\lambda}{2}\right)} \\ &\times \sum_{i=0}^{+\infty}\sum_{l=1}^{u_3} \frac{\lambda^i\, y_{3,l}^{\left(i+\frac{1}{2}\right)} e^{\left(\frac{a}{Kb\rho'}+\frac{1}{2}\right)y_{3,l}}\, \mathrm{Ei}\left(-\frac{1}{K}\left(\frac{ay_{3,l}}{b}+\frac{a}{b\rho'}\right)\right)}{i!2^{2i+\frac{1}{2}}\Gamma\left(i+\frac{1}{2}\right)(u_3+1)^2\big(L_{u_3+1}\big(y_{3,l}\big)\big)^2}, \end{aligned} \tag{22}$$

and

$$R_2 = \frac{1}{K}\sum_{l=1}^{u_4} \frac{x_{4,l}e^{(1-K)x_{4,l}}\log_2\left(1+ax_{4,l}\right)}{\left(u_{4,l}+1\right)^2\big(L_{u_4+1}\big(x_{4,l}\big)\big)^2}, \tag{23}$$

respectively, where the values of a, b and λ are given in (19a), (19b) and (19c), respectively.

5.1.3 Asymptotic SNR analysis

Now, we expatiate on the high-SNR regime, to gain some insights on the results in Sects. 5.1.1 and 5.1.2. For the sake of simplicity, we assume that ρ' grows large.

1 Corollary 1

Suppose that ρ' grows large. The asymptotic SINR and SNR satisfy

$$\lim_{\rho'\to+\infty}\Lambda_1 = \frac{d_{F1}^{-\alpha_1}\left(\sum_{k=1}^{K}|h_k||g_{1,k}|\right)^2}{d_{F2}^{-\alpha_2}\left|\sum_{k=1}^{K}e^{j\theta_k}h_kg_{2,k}\right|^2}, \tag{24}$$

and

$$\lim_{\rho'\to+\infty}\Lambda_2 = +\infty, \tag{25}$$

respectively.

1 ***Proof***

We can easily see that Λ_1 *and* Λ_2 *converge to (24) and (25), respectively.* □

1 Corollary 2

Suppose that ρ' *grow large. The asymptotic OPs satisfy*

$$\lim_{\rho'\to+\infty}\mathbb{P}_1(\tilde{\gamma}_1)=\frac{e^{\left(\frac{1}{Kb}-\frac{\lambda}{2}\right)}}{\sqrt{\frac{2a}{Kb\tilde{\gamma}_1}}}\times\sum_{i=0}^{+\infty}\sum_{j=0}^{+\infty}\frac{\lambda^i(-1)^j\Gamma\left(i+j+\frac{1}{2}\right)}{i!j!2^i\Gamma\left(i+\frac{1}{2}\right)\left(\frac{2a}{Kb\tilde{\gamma}_1}\right)^{(i+j)}}, \tag{26}$$

and

$$\lim_{\rho'\to+\infty}\mathbb{P}_2(\tilde{\gamma}_1,\tilde{\gamma}_2)=1-e^{\left(\frac{1}{Kb}-\frac{\lambda}{2}\right)}\sum_{i=0}^{+\infty}\frac{\lambda^i}{i!2^i}-\left(\frac{e^{\left(\frac{1}{Kb}-\frac{\lambda}{2}\right)}}{\sqrt{\frac{2a}{Kb\tilde{\gamma}_1}}}\times\sum_{i=0}^{+\infty}\sum_{j=0}^{+\infty}\frac{\lambda^i(-1)^j\Gamma\left(i+j+\frac{1}{2}\right)}{i!j!2^i\Gamma\left(i+\frac{1}{2}\right)\left(\frac{2a}{Kb\tilde{\gamma}_1}\right)^{(i+j)}}\right), \tag{27}$$

respectively.

1 ***Proof***

We have

$$\lim_{\rho'\to+\infty}\Gamma\left(i+j+\frac{3}{2},\frac{1}{Kb\rho'}\right)=\lim_{\rho'\to+\infty}\Gamma\left(i+j+\frac{3}{2},\frac{\tilde{\gamma}_2+1}{Kb\rho'}\right)=\Gamma\left(i+j+\frac{3}{2}\right),$$

and

$\lim_{\rho'\to+\infty}e^{-\left(\frac{\tilde{\gamma}_2}{Kb\rho'}+\frac{1}{Kba\rho'}\right)}=1$. Thus, the limits of both $\mathbb{P}_1(\tilde{\gamma}_1)$ and $\mathbb{P}_2(\tilde{\gamma}_1,\tilde{\gamma}_2)$ for $\rho'\to+\infty$ can be obtained as in (26) and (27), respectively. □

To provide more insight on the studied system's performance, we will consider shortly, the high-SNR slope, which is defined as $S=\lim_{\rho'\to\infty}\frac{R(\rho')}{\log_2(\rho')}$ [40]. The asymptotic expression for F1's ER and the ceiling for F2's ER derived in the following corollary will help to obtain it.

1 Corollary 3

Suppose that ρ' *grows large.* R_{F1} *approaches a ceiling that is given by*

$$\lim_{\rho'\to+\infty} R_{F1} = -\frac{1}{K\ln 2}\, e^{-\frac{\lambda}{2}} \times \sum_{i=0}^{+\infty}\sum_{l=1}^{u_3} \frac{\lambda^i\, y_{3,l}^{\left(i+\frac{1}{2}\right)}\, e^{\frac{y_{3,l}}{2}}\, \mathrm{Ei}\left(-\frac{a y_{3,l}}{Kb}\right)}{i!\, 2^{2i+\frac{1}{2}}\, \Gamma\left(i+\frac{1}{2}\right)(u_3+1)^2\left(L_{u_3+1}\left(y_{3,l}\right)\right)^2}, \tag{28}$$

and the tight upper bound of R_{F2}'s high-SNR approximation is expressed as

$$R_{F2}^{\infty} = \log_2\left(b\rho' K\right). \tag{29}$$

1 ***Proof***

For F1, we have $\lim_{\rho'\to+\infty} e^{\frac{a}{Kb\rho'}} = \lim_{\rho'\to+\infty} e^{\frac{a}{Kb\rho' y_{3,l}}} = 1$, *and*

$\lim_{\rho'\to+\infty} \mathrm{Ei}\left(-\frac{1}{K}\left(\frac{a y_{3,l}}{b} + \frac{a}{b\rho'}\right)\right) = \mathrm{Ei}\left(-\frac{a}{Kb} y_{3,l}\right)$. Thus, the limit of R_{F1} for $\rho' \to +\infty$ can be obtained as in (28).

For F2, since $\log_2(1 + b\rho' X)$ with respect to X is concave, so by considering Jensen's inequality [41], we have

$$R_{F2} = \mathbb{E}\left(\log_2\left(1 + b\rho' X\right)\right) \le \log_2\left(1 + b\rho' \mathbb{E}(X)\right) = \log_2\left(1 + b\rho' K\right).$$

When $\rho' \to +\infty$, we obtain (29). □

1 Corollary 4

In the analyzed uplink RIS-NOMA network, the high-SNR slopes of F1 and F2 are given by $\mathcal{S}_1 = 0$ *and* $\mathcal{S}_2 = 1$, *respectively.*

1 ***Proof***

We have

$$\mathcal{S}_1 = \lim_{\rho'\to+\infty} \frac{R_1(\rho')}{\log_2(\rho')} = \rho' \ln(2) \frac{d\, R_1^{+\infty}}{d\rho'} = 0,$$

and

$$\mathcal{S}_2 = \lim_{\rho'\to+\infty} \frac{R_2(\rho')}{\log_2(\rho')} = \rho' \ln(2) \frac{d\, R_2^{+\infty}}{d\rho'} = 1.$$

□

The diversity order analysis shows that F2 attains higher reliability ($d_2 = 1$) than F1 ($d_1 = 0$) in the high-SNR regime. This contrast arises because F1 remains interference-limited due to residual interference from F2's signal, while F2 enjoys interference-free decoding once SIC is successfully applied. As a result, the OP of F2 decreases more rapidly with increasing SNR, whereas F1's performance eventually saturates. This behavior

highlights an inherent design trade-off between rate and reliability in RIS–NOMA systems.

1 Corollary 5

The diversity orders for users F1 and F2 in the high-SNR regime are given by:

$$d_{\mathrm{F1}} = 0 \quad \text{(F1 - Prioritized User)} \tag{30}$$

$$d_{\mathrm{F2}} = 1 \quad \text{(F2 - Secondary User)} \tag{31}$$

1 ***Proof***

The diversity order is defined as $d = -\lim_{\rho' \to \infty} \frac{\log P_{\mathrm{out}}(\gamma_{\mathrm{th}})}{\log \rho'}$. *For F1, from asymptotic OP expression (34),* $P_{\mathrm{F1}}^{\infty} = C_1$ *(independent of* ρ'*), yielding* $d_{\mathrm{F1}} = 0$. *For F2, from asymptotic OP expression (35),* $P_{\mathrm{F2}}^{\infty} = \frac{\tilde{\gamma}_2}{Kb\rho'} + \mathcal{O}(\rho'^{-2})$, *yielding* $d_{\mathrm{F2}} = 1$. □

1 ***Remark 3***

The diversity analysis highlights a key trade-off: coherent beamforming (F1) offers array gain but yields zero diversity because its performance saturates under interference, whereas random phase-shifting (F2) achieves unit diversity through interference-free decoding after SIC. This distinction guides practical deployment decisions: ultra-reliable low-latency communications (URLLC) should leverage F2's position for improved reliability, while enhanced mobile broadband (eMBB) services can benefit from F1's position for higher throughput. Dynamic user pairing is therefore advisable in quality of service (QoS)-aware systems.

5.2 The RIS-OMA case

When considering a RIS-OMA network, the received signals from F1 and F2 at the BS are given by

$$y_1^{\mathrm{OMA}} = (\mathbf{h}\Theta\mathbf{g}_1) d_1^{-\frac{\alpha_1}{2}} d_3^{-\frac{\alpha_3}{2}} \sqrt{P} s_1 + n, \tag{32}$$

and

$$y_2^{\mathrm{OMA}} = (\mathbf{h}\Theta\mathbf{g}_2) d_2^{-\frac{\alpha_2}{2}} d_3^{-\frac{\alpha_3}{2}} \sqrt{P} s_2 + n, \tag{33}$$

respectively. At the BS, the signals received from F1 and F2 are decoded separately and the corresponding SNRs are given by

$$\Lambda_1^{\mathrm{OMA}} = d_1^{-\frac{\alpha_1}{2}} d_3^{-\frac{\alpha_3}{2}} |\mathbf{h}\Theta\mathbf{g}_1|^2 \rho', \tag{34}$$

and

$$\Lambda_2^{\mathrm{OMA}} = d_2^{-\frac{\alpha_2}{2}} d_3^{-\frac{\alpha_3}{2}} |\mathbf{h}\Theta\mathbf{g}_2|^2 \rho', \tag{35}$$

respectively. The achievable data rates of F1 and F2 under the OMA scheme are given by $\frac{1}{2}\log_2\left(1 + d_1^{-\alpha_1} d_3^{-\alpha_3} \beta^2 \left(\sum_{k=1}^{K} |h_k||g_{1,k}|\right)^2 \rho'\right)$ and $\frac{1}{2}\log_2\left(1 + d_2^{-\alpha_2} d_3^{-\alpha_3} \beta^2 \left|\sum_{k=1}^{K} e^{j\theta_k} h_k g_{2,k}\right|^2 \rho'\right)$, respectively. Here, for a fair comparison, we presume that every UE utilizes half of the available resource block.

5.2.1 OPs

1 Theorem 6

When F1 and F2 are under the OMA scheme, their OPs are given by

$$^{\mathrm{OMA}}\mathbb{P}_1\left(\tilde{\gamma}_1^0\right) = e^{-\frac{\lambda}{2}} \sum_{i=0}^{+\infty} \frac{\lambda^i \gamma\left(i + \frac{1}{2}, \frac{\tilde{\gamma}_1^0}{2a\rho'}\right)}{i! 2^i \Gamma\left(i + \frac{1}{2}\right)}, \tag{36}$$

and

$$^{\mathrm{OMA}}\mathbb{P}_2\left(\tilde{\gamma}_2^0\right) = 1 - e^{-\frac{1}{K}}\left(\frac{\tilde{\gamma}_2^0}{b\rho'}\right), \tag{37}$$

respectively, where $\tilde{\gamma}_1^o = 2^{2\tilde{R}_1} - 1$ *and* $\tilde{\gamma}_2^o = 2^{2\tilde{R}_2} - 1$.

1 *Proof*

$^{\mathrm{OMA}}\mathbb{P}_1\left(\tilde{\gamma}_1^0\right)$ *and* $^{\mathrm{OMA}}\mathbb{P}_2\left(\tilde{\gamma}_2^0\right)$ *can be easily derived as follows:*

$$^{\mathrm{OMA}}\mathbb{P}_1\left(\tilde{\gamma}_1^0\right) = \Pr\left(\mathrm{a}\rho'\mathrm{Y} < \tilde{\gamma}_1^{\mathrm{o}}\right) = \mathrm{F}_{\mathrm{Y}}\left(\frac{\tilde{\gamma}_1^{\mathrm{o}}}{\mathrm{a}\rho'}\right), \tag{38}$$

and

$$^{\mathrm{OMA}}\mathbb{P}_2\left(\tilde{\gamma}_2^0\right) = \Pr\left(\mathrm{a}\rho'\mathrm{X} < \tilde{\gamma}_2^{\mathrm{o}}\right) = \mathrm{F}_{\mathrm{X}}\left(\frac{\tilde{\gamma}_2^{\mathrm{o}}}{\mathrm{a}\rho'}\right). \tag{39}$$

□

5.2.2 ERs

Given the SNRs in (34) and (35), the ERs of F1 and F2 under the OMA scheme are given by

$$^{\mathrm{OMA}}R_1 = \frac{1}{2}\mathbb{E}\Big(\log_2\Big(1+\Lambda_1^{\mathrm{OMA}}\Big)\Big), \tag{40}$$

and

$$^{\mathrm{OMA}}R_2 = \frac{1}{2}\mathbb{E}\Big(\log_2\Big(1+\Lambda_2^{\mathrm{OMA}}\Big)\Big), \tag{41}$$

respectively.

Using Theorem 4 and 5, $^{\mathrm{OMA}}R_1$ and $^{\mathrm{OMA}}R_2$ are expressed as

$$\begin{aligned} ^{\mathrm{OMA}}R_1 \approx{}& \frac{\lambda^{\frac{1}{4}}e^{-\frac{\lambda}{2}}}{4} \\ &\times\sum_{l=1}^{u_5}\frac{y_{5,l}^{\frac{3}{4}}e^{\frac{y_{5,l}}{2}}I_{-\frac{1}{2}}\left(\sqrt{\lambda y_{5,l}}\right)\log_2\left(1+a\rho' y_{5,l}\right)}{\left(u_{5,l}+1\right)^2\left(L_{u_5+1}\left(y_{5,l}\right)\right)^2}, \end{aligned} \tag{42}$$

and

$$^{\mathrm{OMA}}R_2 \approx \frac{1}{2K}\sum_{l=1}^{u_4}\frac{x_{4,l}e^{(1-K)x_{4,l}}\log_2\left(1+b\rho' x_{4,l}\right)}{\left(u_{4,l}+1\right)^2\left(L_{u_4+1}\left(x_{4,l}\right)\right)^2}, \tag{43}$$

respectively.

5.2.3 Asymptotic SNR analysis

Now, to get further insights on the results in subsections 5.2.1 and 5.2.2, we elaborate on the high-SNR regime.

1 Corollary 6

Suppose that ρ' grow large. The asymptotic OPs in a OMA scheme satisfy

$$\begin{aligned} ^{\mathrm{OMA}}\mathbb{P}_1^{\infty} &= \lim_{\rho\to+\infty} {}^{\mathrm{OMA}}\mathbb{P}_1 \\ &= e^{-\frac{\lambda}{2}} \\ &\times\sum_{i=0}^{+\infty}\frac{\lambda^i}{i!2^i\Gamma\left(i+\frac{3}{2}\right)}\left(\frac{\tilde{\gamma}_1^0}{2a\rho'}\right)^{i+\frac{1}{2}}, \end{aligned} \tag{44}$$

and

$$^{\mathrm{OMA}}\mathbb{P}_2^{\infty} = \lim_{\rho'\to+\infty} {}^{\mathrm{OMA}}\mathbb{P}_2 = 1, \tag{45}$$

respectively.

1 *Proof*

Considering the fact that $\gamma(s,z)$ behaves near $z=0$ asymptotically like $\gamma(s,z)\approx\frac{z^s}{s}$, (44) can be easily obtained.